Eur. Phys. J. C 21, 599–606 (2001)
Digital Object Identifier (DOI) 10.1007/s100520100765

THE EUROPEAN PHYSICAL JOURNAL C

Multiplicity of charged and neutral pions in deep-inelastic scattering of 27.5 GeV positrons on hydrogen

The HERMES Collaboration

A. Airapetian[31], N. Akopov[31], Z. Akopov[31], M. Amarian[23,26,31], J. Arrington[2], E.C. Aschenauer[7,13,23], H. Avakian[11], R. Avakian[31], A. Avetissian[31], E. Avetissian[31], P. Bailey[15], B. Bains[15], C. Baumgarten[21], M. Beckmann[12], S. Belostotski[24], S. Bernreuther[9], N. Bianchi[11], H. Böttcher[7], A. Borissov[6,14], M. Bouwhuis[15], J. Brack[5], S. Brauksiepe[12], B. Braun[9,21], W. Brückner[14], A. Brüll[14,18], P. Budz[9], H.J. Bulten[17,23,30], G.P. Capitani[11], P. Carter[4], P. Chumney[22], E. Cisbani[26], G.R. Court[16], P.F. Dalpiaz[10], R. De Leo[3], L. De Nardo[1], E. De Sanctis[11], D. De Schepper[2,18], E. Devitsin[20], P.K.A. de Witt Huberts[23], P. Di Nezza[11], V. Djordjadze[7], M. Düren[9], A. Dvoredsky[4], G. Elbakian[31], J. Ely[5], A. Fantoni[11], A. Fechtchenko[8], M. Ferro-Luzzi[23], K. Fiedler[9], B.W. Filippone[4], H. Fischer[12], B. Fox[5], J. Franz[12], S. Frullani[26], Y. Gärber[7], F. Garibaldi[26], E. Garutti[23], G. Gavrilov[24], V. Gharibyan[31], A. Golendukhin[6,21,31], G. Graw[21], O. Grebeniouk[24], P.W. Green[1,28], L.G. Greeniaus[1,28], A. Gute[9], W. Haeberli[17], M. Hartig[28], D. Hasch[7,11], D. Heesbeen[23], F.H. Heinsius[12], M. Henoch[9], R. Hertenberger[21], W.H.A. Hesselink[23], P. Hoffmann-Rothe[23], G. Hofman[5], Y. Holler[6], R.J. Holt[15], B. Hommez[13], W. Hoprich[14], G. Iarygin[8], H. Ihssen[6,23], M. Iodice[26], A. Izotov[24], H.E. Jackson[2], A. Jgoun[24], R. Kaiser[7,27,28], J. Kanesaka[29], E. Kinney[5], A. Kisselev[24], P. Kitching[1], H. Kobayashi[29], N. Koch[9], K. Königsmann[12], H. Kolster[21,23], V. Korotkov[7], E. Kotik[1], V. Kozlov[20], V.G. Krivokhijine[8], G. Kyle[22], L. Lagamba[3], A. Laziev[23], P. Lenisa[10], T. Lindemann[6], W. Lorenzon[19], N.C.R. Makins[2,15], J.W. Martin[18], H. Marukyan[31], F. Masoli[10], M. McAndrew[16], K. McIlhany[4,18], R.D. McKeown[4], F. Meissner[7,21], F. Menden[12], A. Metz[21], N. Meyners[6], O. Mikloukho[24], C.A. Miller[1,28], R. Milner[18], V. Muccifora[11], R. Mussa[10], A. Nagaitsev[8], E. Nappi[3], Y. Naryshkin[24], A. Nass[9], W.-D. Nowak[7], T.G. O'Neill[2], R. Openshaw[28], J. Ouyang[28], B.R. Owen[15], S.F. Pate[18,22], S. Potashov[20], D.H. Potterveld[2], G. Rakness[5], R. Redwine[18], D. Reggiani[10], A.R. Reolon[11], R. Ristinen[5], K. Rith[9], D. Robinson[15], A. Rostomyan[31], M. Ruh[12], D. Ryckbosch[13], Y. Sakemi[29], F. Sato[29], I. Savin[8], C. Scarlett[19], A. Schäfer[25], C. Schill[12], F. Schmidt[9], M. Schmitt[9], G. Schnell[22], K.P. Schüler[6], A. Schwind[7], J. Seibert[12], T.-A. Shibata[29], T. Shin[18], V. Shutov[8], M.C. Simani[10,23,30], A. Simon[12], K. Sinram[6], E. Steffens[9], J.J.M. Steijger[23], J. Stewart[16,28], U. Stösslein[7], K. Suetsugu[29], M. Sutter[18], H. Tallini[16], S. Taroian[31], A. Terkulov[20], S. Tessarin[10], E. Thomas[11], B. Tipton[18,4], M. Tytgat[13], G.M. Urciuoli[26], J.F.J. van den Brand[23,30], G. van der Steenhoven[23], R. van de Vyver[13], J.J. van Hunen[23], M.C. Vetterli[27,28], V. Vikhrov[24], M.G. Vincter[1,28], J. Visser[23], E. Volk[14], C. Weiskopf[9], J. Wendland[27,28], J. Wilbert[9], T. Wise[17], K. Woller[6], S. Yoneyama[29], H. Zohrabian[31]

[1] Department of Physics, University of Alberta, Edmonton, Alberta T6G 2J1, Canada
[2] Physics Division, Argonne National Laboratory, Argonne, IL 60439-4843, USA
[3] Istituto Nazionale di Fisica Nucleare, Sezione di Bari, 70124 Bari, Italy
[4] W.K. Kellogg Radiation Laboratory, California Institute of Technology, Pasadena, CA 91125, USA
[5] Nuclear Physics Laboratory, University of Colorado, Boulder, CO 80309-0446, USA
[6] DESY, Deutsches Elektronen Synchrotron, 22603 Hamburg, Germany
[7] DESY Zeuthen, 15738 Zeuthen, Germany
[8] Joint Institute for Nuclear Research, 141980 Dubna, Russia
[9] Physikalisches Institut, Universität Erlangen-Nürnberg, 91058 Erlangen, Germany
[10] Istituto Nazionale di Fisica Nucleare, Sezione di Ferrara and Dipartimento di Fisica, Università di Ferrara, 44100 Ferrara, Italy
[11] Istituto Nazionale di Fisica Nucleare, Laboratori Nazionali di Frascati, 00044 Frascati, Italy
[12] Fakultät für Physik, Universität Freiburg, 79104 Freiburg, Germany
[13] Department of Subatomic and Radiation Physics, University of Gent, 9000 Gent, Belgium
[14] Max-Planck-Institut für Kernphysik, 69029 Heidelberg, Germany
[15] Department of Physics, University of Illinois, Urbana, IL 61801, USA
[16] Physics Department, University of Liverpool, Liverpool L69 7ZE, UK
[17] Department of Physics, University of Wisconsin-Madison, Madison, WI 53706, USA
[18] Laboratory for Nuclear Science, Massachusetts Institute of Technology, Cambridge, MA 02139, USA
[19] Randall Laboratory of Physics, University of Michigan, Ann Arbor, MI 48109-1120, USA
[20] Lebedev Physical Institute, 117924 Moscow, Russia
[21] Sektion Physik, Universität München, 85748 Garching, Germany

[22] Department of Physics, New Mexico State University, Las Cruces, NM 88003, USA
[23] Nationaal Instituut voor Kernfysica en Hoge-Energiefysica (NIKHEF), 1009 DB Amsterdam, The Netherlands
[24] Petersburg Nuclear Physics Institute, St. Petersburg, Gatchina, 188350 Russia
[25] Institut für Theoretische Physik, Unversität Regensburg, 93040 Regensburg, Germany
[26] Istituto Nazionale di Fisica Nucleare, Sezione Roma 1 - Gruppo Sanità and Physics Laboratory, Istituto Superiore di Sanità, 00161 Roma, Italy
[27] Department of Physics, Simon Fraser University, Burnaby, British Columbia V5A 1S6, Canada
[28] TRIUMF, Vancouver, British Columbia V6T 2A3, Canada
[29] Department of Physics, Tokyo Institute of Technology, Tokyo 152, Japan
[30] Department of Physics and Astronomy, Vrije Universiteit, 1081 HV Amsterdam, The Netherlands
[31] Yerevan Physics Institute, 375036, Yerevan, Armenia

Received: 2 April 2001 / Revised version: 27 June 2001 /
Published online: 7 September 2001 –

Abstract. Measurements of the individual multiplicities of π^+, π^- and π^0 produced in the deep-inelastic scattering of 27.5 GeV positrons on hydrogen are presented. The average charged pion multiplicity is the same as for neutral pions, up to $z \approx 0.7$, where z is the fraction of the energy transferred in the scattering process carried by the pion. This result (below $z \approx 0.7$) is consistent with isospin invariance. The total energy fraction associated with charged and neutral pions is $0.51 \pm 0.01(\text{stat.}) \pm 0.08$ (syst.) and $0.26 \pm 0.01(\text{stat.}) \pm 0.04(\text{syst.})$, respectively. For fixed z, the measured multiplicities depend on both the negative squared four momentum transfer Q^2 and the Bjorken variable x. The observed dependence on Q^2 agrees qualitatively with the expected behaviour based on NLO-QCD evolution, while the dependence on x is consistent with that of previous data after corrections have been made for the expected Q^2-dependence.

1 Introduction

The semi-inclusive production of pseudoscalar mesons in Deep-Inelastic Scattering (DIS) is a good tool to test the quark-parton model and QCD. A schematic diagram and the relevant variables for the process are shown in Fig. 1. In the proton rest frame, the energy of the exchanged virtual photon γ^* is $\nu = E - E'$ (E and E' being the energies of the incident and scattered positrons respectively), while its squared four-momentum is $-Q^2$. The quantity $x = Q^2/2M\nu$, where M is the proton mass, is the fraction of the light-cone momentum of the nucleon carried by the struck quark. The parton distribution function q_f describes the momentum distribution of quarks in the nucleon, while the fragmentation function D_f^π is a measure of the probability that a quark of flavour f fragments into a pion of energy $E_\pi = z\nu$. The quantity $d\sigma_f$ is the cross-section for the absorption of the virtual photon by the struck quark. The quantity of interest in this paper is the pion differential multiplicity, or the number (N^π) of pions produced in DIS, normalised to the total number (N_{DIS}) of inclusive DIS events ($e + p \to e' + X$). In the QCD improved quark-parton model, it is given by the expression:

$$\frac{1}{N_{DIS}(Q^2)}\frac{dN^\pi(z,Q^2)}{dz} = \frac{\sum_f e_f^2 \int_0^1 dx\; q_f(x,Q^2) D_f^\pi(z,Q^2)}{\sum_f e_f^2 \int_0^1 dx\; q_f(x,Q^2)}, \qquad (1)$$

where the sum is over quarks and antiquarks of flavour f, and e_f is the quark charge in units of the elementary charge. Perturbative QCD calculations in leading [1, 2] and next-to-leading order [3–9] suggest a significant

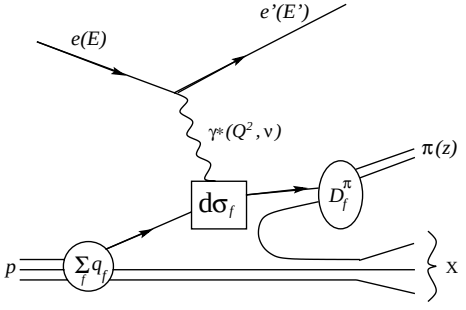

Fig. 1. Semi-inclusive pion electroproduction diagram

Q^2-dependence of the fragmentation process. These QCD expectations have been verified by experimental results of hadron production in e^+e^- collisions (see references to experiments in [7–9]), and in lepton-nucleon scattering at large ν and Q^2 [10–17]. Data with pions identified in the final state are also available [18–22]. This paper presents measurements at lower Q^2 of multiplicities for both charged and neutral pions as a function of the variable z in the range $0.1 \le z \le 0.9$. This study of the Q^2-dependence above 1 GeV^2 provides new and precise information on the scaling violation of the pion fragmentation process at relatively small values of W (3.1 GeV $\le W \le$ 6.6 GeV) [23]; W is the invariant mass of the virtual-photon + proton system.

Evidence for an additional x or W dependence of the multiplicities has been seen by previous experiments [10–12]. This has been ignored in the formalism leading to (1). The multiplicities measured at HERMES were also studied as a function of x to determine whether they show a similar behaviour. Also, charged and neutral pion multiplicities are compared as a test of isospin invariance.

2 Experiment

The measurements described here were performed with the HERMES spectrometer [24] using the 27.5 GeV positron beam stored in the HERA ring at DESY. The spectrometer consists of two identical halves above and below the positron and proton beam pipes. The beam with a typical current in the range between 10 and 35 mA was incident on a hydrogen internal gas target [25]. The data used in this analysis were collected during the 1996 and 1997 HERA beam periods. The target was operated in both unpolarised and longitudinally polarised configurations, with typical areal densities of 8×10^{14} and 7×10^{13} atoms/cm^2, respectively. The data from the polarised target were analysed by averaging over the two spin orientations, producing results that are consistent with those from the unpolarised target.

The scattered positrons and any resulting hadrons were detected simultaneously by the HERMES spectrometer. The geometrical acceptance of the spectrometer is $\pm$(40 - 140) mrad in the vertical direction and $\pm$170 mrad in the horizontal direction.

The identification of the scattered positron was accomplished using a gas threshold Čerenkov counter, a transition radiation detector, a scintillator hodoscope preceded by two radiation lengths of lead (preshower counter), and an electromagnetic calorimeter. This system provided positron identification with an average efficiency of 98% and a hadron contamination of less than 1%. Events were selected by imposing the kinematic restrictions $Q^2 \geq 1$ GeV^2 and $y \leq 0.85$, where $y = \nu/E$ is the virtual photon fractional energy.

The Čerenkov counter was filled with a mixture of 70% nitrogen and 30% perfluorobutane (C_4F_{10}), providing a momentum threshold of 3.8, 13.6 and 25.8 GeV for pions, kaons, and protons respectively. The momentum was restricted to the range between 4.5 GeV and 13 GeV in the data analysis to eliminate possible kaon or proton contamination of the charged pion sample. The contribution from the inefficiency of the Čerenkov detector to the systematic uncertainty on the charged pion multiplicities was evaluated to be 3.2% [26].

The electromagnetic calorimeter is composed of 840 F101 lead glass blocks [27], and provided neutral pion identification by the detection of the two neutral clusters from two-photon π^0 decay. Each of the two clusters was required to have an energy $E_\gamma \geq 1.4$ GeV. The measurement of both the energies ($E_{\gamma 1}$ and $E_{\gamma 2}$) and the relative angle ($\Theta_{\gamma\gamma}$) of the two photons allowed the reconstruction of the invariant mass $m_{\gamma\gamma} = \sqrt{4E_{\gamma 1}E_{\gamma 2}\sin^2(\Theta_{\gamma\gamma}/2)}$. A typical measured spectrum of $m_{\gamma\gamma}$ is shown in Fig. 2. The distribution is centered at $m_{\gamma\gamma} = 0.1348 \pm 0.0008$ GeV. The good π^0 mass resolution of about 0.012 GeV allowed a safe background subtraction. The background was evaluated in each kinematic bin by fitting the invariant mass spectrum with a Gaussian plus a polynomial that reproduces well the shape of the background due to uncorrelated photons. The relevant contribution to the systematic uncertainty is less than 2%. It was evaluated by repeating the fitting procedure for different ranges and with polynomials of different order [23]. The number of π^0 detected was obtained by integrating the peak corrected for background, over the range $\pm2.5\sigma$ around the centroid of the Gaussian.

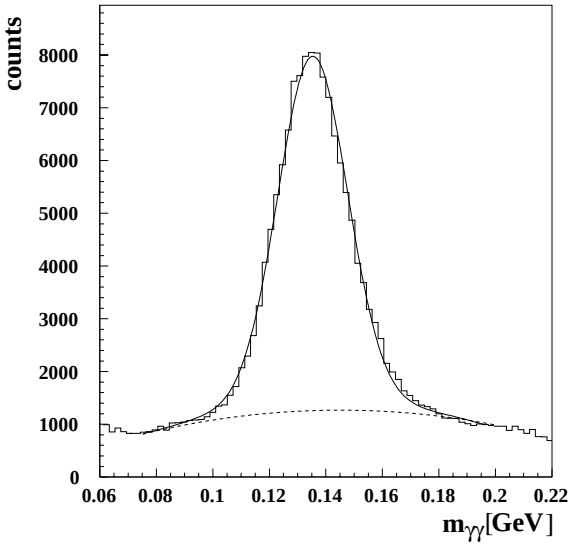

Fig. 2. Two-photon invariant mass spectrum. The solid line is a fit with a Gaussian plus a polynomial. The dashed line represents the background only

In order to exclude effects from nucleon resonances as well as kinematic regions with inadequate geometrical acceptance, the additional requirement $W^2 \geq 10$ GeV^2 was imposed for this analysis. This also helps to select hadrons originating from fragmentation of the struck quark, by excluding the kinematic region in which current and target fragments are not well separated. Fragments from the target remnant are already strongly reduced due to the forward angle acceptance of the HERMES spectrometer.

After background subtraction and data quality plus kinematic cuts, a total of 4.2×10^5 (1.3×10^5) semi-inclusive charged (neutral) pions were considered in the analysis.

The HERMES Monte Carlo program (HMC) was used to evaluate the detection probability for pions produced in DIS events. HMC is based on the LEPTO event generator [28], the LUND fragmentation model [29], and on the GEANT3 code for the simulation of the detector response [30]. The LUND parameters were adjusted to fit various kinematic distributions from HERMES semi-inclusive data [31]. As an example, Fig. 3 shows comparisons between the measured energy spectra of charged and neutral pions and the relevant HMC simulations. The agreement in the shape of the spectra is reasonable. The energy range of the charged pions is smaller than for neutral pions due to the stronger kinematic restriction imposed on the data to ensure good charged pion identification.

The detection probability of the pions produced in detected DIS events is shown as a function of z in Fig. 4. This quantity was computed using HMC to account for effects from pion losses due to the finite angular acceptance of the spectrometer, from detector inefficiencies, and from fiducial cuts imposed in the data analysis. A probability

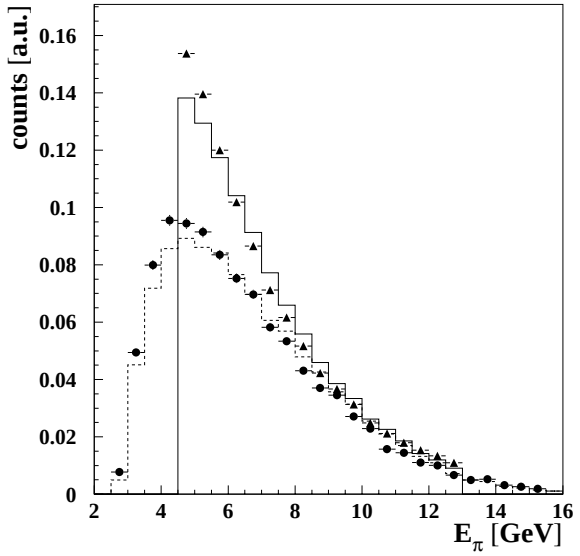

Fig. 3. Comparison between the measured and simulated pion energy spectra. Filled circles (triangles) are the neutral (charged) pion measurements. The histograms are the simulated spectra for neutral (dashed line) and charged (full line) pions. All spectra have been normalized to unit area

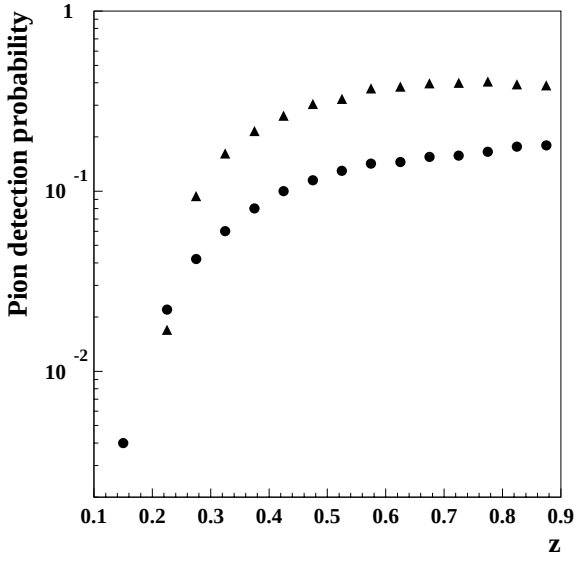

Fig. 4. Detection probability as a function of z for charged (triangles) and neutral (circles) pions when the DIS positron is detected

up to ∼40% is obtained for charged pions in the intermediate and high z-region. At low z the detection probability for charged pions is further reduced due to the restriction on the pion momentum range. The probability for neutral pions is lower due to the need to detect both of the decay photons. Since the angle of these two photons is correlated with the π^0 energy, the detection probability strongly increases with z, reaching ∼18% in the highest z-bin. The positron detection probability does not affect the multiplicity defined in (1). Smearing by instrumental resolution of the positron kinematics in the various ν-bins was included in the Monte Carlo. This effect also leads to migration of events in z. Corrections due to smearing vary from ∼2% in the lowest z-bin to 30-35% in the highest z-bin. The systematic uncertainty on the multiplicities due to the detection probability (including smearing) is 7.5% (4.5%) for neutral (charged) pions. It was evaluated with HMC by drastically restricting the geometrical cuts or the allowed ranges of the relevant kinematic variables. The multiplicities plotted in this paper were corrected for the effects described above.

Radiative corrections for internal bremsstrahlung processes were applied. These corrections range from ∼3% in the lowest z-bin to ∼15% in the highest z-bin, and result in a systematic uncertainty on the multiplicities of less than 1%. Radiative corrections for external bremsstrahlung processes in the target were found to be negligible due to the small thickness of the hydrogen gas target [32].

It has been determined from Monte Carlo studies that diffractive production of pions is negligible ($< 2\%$) in the HERMES kinematic range, and so no correction was made for this contribution.

3 Results

Under the assumption of isospin invariance, the quark-parton model predicts that the multiplicity for neutral pions is equal to the average of those for positive and negative pions. Specifically, the fragmentation function $D_f^{\pi^0}$ is assumed equal to the average of the two charged pion fragmentation functions $D_f^{\pi^+}$ and $D_f^{\pi^-}$, because the quark content of the π^0 is the same as the average of π^+ and π^- [1]. The multiplicities $\frac{1}{N_{DIS}}\frac{dN^{\pi^0}}{dz}$ and $\frac{1}{N_{DIS}}[\frac{dN^{\pi^+}}{dz} + \frac{dN^{\pi^-}}{dz}]/2$, are plotted as a function of z in Fig. 5a. Numerical values are given in Table 1, where the individual multiplicities for π^+ and π^- are also listed, along with the ranges and average values of the relevant kinematic variables. Both data sets in Fig. 5a show a strong decrease with the z variable that can be parameterized with the expression [7]

$$\frac{1}{N_{DIS}}\frac{dN^{\pi}}{dz} = Nz^{\alpha}(1-z)^{\beta}. \qquad (2)$$

The dashed curve shown in Fig. 5a is a Q^2 independent fit to the π^0 data using the above expression ($N = 0.335$, $\alpha = -1.371$, $\beta = 1.167$). Also shown in Fig. 5a is another Q^2-independent parameterization using the independent fragmentation model. The coefficients of this parameterization were obtained in Ref. [33] by tuning on old data at Q^2-values close to that of HERMES (see [33] for references to these data). This parameterization reproduces the behaviour of the present data fairly well, apart from the high z-region. As expected from isospin invariance, the agreement between the data for neutral and charged pions is excellent, at least up to $z \sim 0.70$ as shown by the ratio

[1] $\pi^0 = \frac{1}{\sqrt{2}}(u\bar{u} - d\bar{d})$; $\pi^+ = u\bar{d}$; $\pi^- = d\bar{u}$

in Fig. 5b, which is consistent with unity below $z \sim 0.70$. The verification of isospin invariance agrees with the conclusion from earlier studies by BEBC, which used neutrino scattering [16,17], and by EMC [18]. In the latter analysis, however, charged hadrons were compared with neutral pions. The current data show that at higher z, the multiplicity is larger for charged pions than for neutral pions. This difference suggests a possible contribution, via the radiative tail and instrumental resolution, from exclusive processes (e.g. $\gamma^* + p \to \pi^+ + \Delta^0$) where resonances affect each isospin channel differently. A recent calculation [34] of hard exclusive electroproduction indeed predicts an enhancement of charged over neutral pion production of roughly an order of magnitude. Higher twist processes could also play a role at high z [35]. Furthermore, E665 sees a significant contribution from diffractive processes at $x_F > 0.75$ [2], although the kinematics of this experiment, notably W, are very different [15]. The excess of charged over neutral pions at high z is being investigated further.

Comparison of results obtained with unpolarised and polarised targets and of those with the top half and the bottom half of the spectrometer resulted in consistency within 3.5% and 2.5% respectively. It should be noted that the data sets for charged and neutral pions were obtained with very different event reconstruction procedures, detection efficiencies and background conditions. Hence the contributions to the systematic uncertainty are quite different for the two cases. The overall systematic uncertainty was estimated to be less than 9% (7%) for neutral (charged) pion electroproduction. The systematic uncertainty on the ratio plotted in Fig. 5b is 6%.

The fraction of the energy ν of the virtual photon transfered to pions

$$\int_0^1 z \frac{1}{N_{DIS}} \frac{dN^\pi}{dz} dz \qquad (3)$$

is $0.26 \pm 0.01(\text{stat.}) \pm 0.04(\text{syst.})$ and $0.51 \pm 0.01(\text{stat.}) \pm 0.08(\text{syst.})$, for the neutral and charged cases, respectively. The corresponding number for neutral pions measured by EMC [18] is $0.27 \pm 0.02 \pm 0.05$. The current results indicate that the fraction of total energy carried by hadrons heavier than pions (mainly K^+, K^-, p, $\bar{p}$) is only $\sim 23\%$. The integrals of (3) were evaluated by adding estimates of the contributions from the unmeasured z-regions to those from the measured z-region, the latter contributions being $0.19 \pm 0.01(\text{stat.}) \pm 0.017(\text{syst.})$ for neutral and $0.28 \pm 0.01(\text{stat.}) \pm 0.02(\text{syst.})$ for charged pions. This extrapolation was based on the z-dependence given by the fit of ref. [33] (solid line in Fig. 5a). The total systematic uncertainty includes an estimate of the error in the extrapolation evaluated by comparing these results with those obtained using the fit of (2). This contribution, 14% (13%) for charged (neutral) pions, dominates the overall systematic uncertainty. It is assumed in estimating this error that the models used are a reasonable representation of the data, even at small z. The possibility of a radically different behaviour of the multiplicities at small z is not accounted for in the systematic uncertainty.

[2] The variable x_F is in practice nearly equal to z

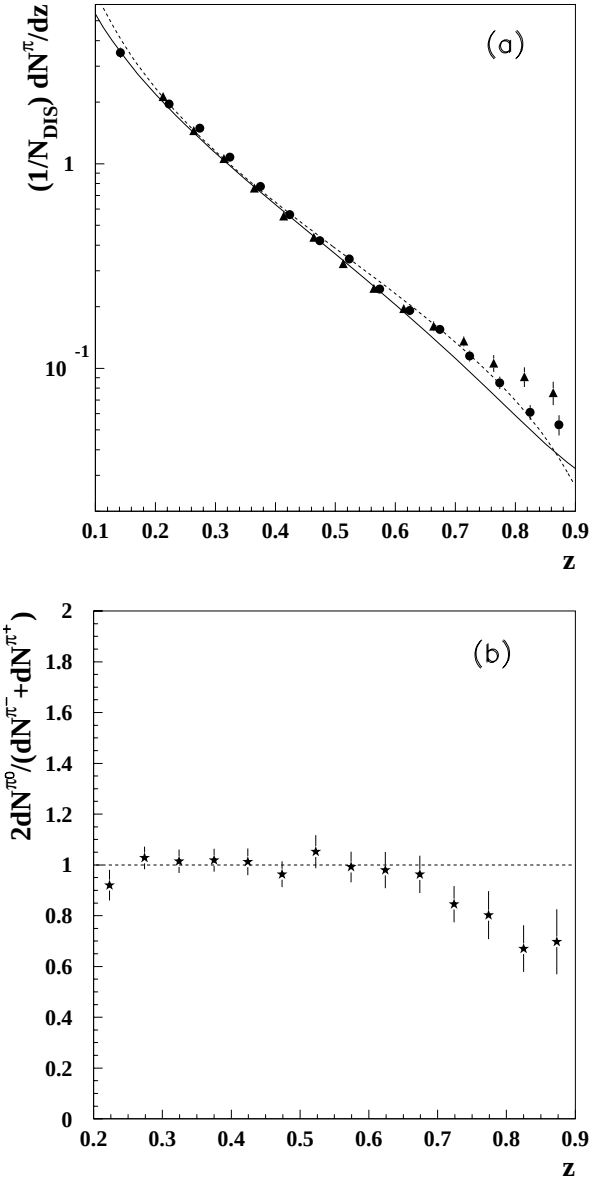

Fig. 5. a Neutral (circles) and average charged (triangles) pion multiplicities. The error bars show the statistical uncertainty only. The systematic uncertainty for the charged (neutral) pions is 7% (9%). The solid line is a parameterization using the independent fragmentation model [33]. The dashed line is a fit to the present neutral pion data using the parameterization given in the text. The charged pion data have been shifted slightly in z to make them visible. **b** Ratio of neutral to average charged pion multiplicities. The systematic uncertainty on the ratio (not included in the error bar) is 6%

In Fig. 6a the HERMES results for the multiplicity of neutral pions as a function of z are compared with previous results from EMC [18] and from SLAC [19]. Figure 6b compares HERMES results for the average charged pion multiplicity with fragmentation function data from EMC [20]. The HERMES results for both neutral and charged pions are systematically higher than those from EMC. This difference can be explained by the different

Table 1. Measured π^0, $(\pi^+ + \pi^-)/2$, π^+, and π^-, multiplicities for various z-bins. The average kinematic variables for this experiment are: E_{beam} = 27.5 GeV, $\sqrt{s}$ = 7.48 GeV, $\langle Q^2 \rangle$ = 2.5 GeV^2, $\langle W^2 \rangle$ = 28.6 GeV^2, $\langle \nu \rangle$ = 16.1 GeV, $\langle x \rangle$ = 0.082, while the ranges are Q^2= [1, $\sim$ 15] GeV^2, W^2= [10, $\sim$ 44] GeV^2, ν= [$\sim$ 5.4, 23.4] GeV, and x= [0.03, $\sim$ 0.6]. The quoted uncertainties are statistical. The systematic uncertainty for the charged (neutral) pions is 7% (9%)

z	$\frac{1}{N^{DIS}} N^{\pi^0}$	$\frac{1}{N^{DIS}} \frac{N^{\pi^+}+N^{\pi^-}}{2}$	$\frac{1}{N^{DIS}} N^{\pi^+}$	$\frac{1}{N^{DIS}} N^{\pi^-}$
0.142	3.39±0.21	-	-	-
0.223	1.96±0.08	2.13±0.11	2.22±0.07	2.04±0.08
0.274	1.49±0.05	1.45±0.04	1.63±0.02	1.28±0.02
0.324	1.075±0.038	1.06±0.03	1.22±0.02	0.897±0.023
0.375	0.774±0.028	0.760±0.022	0.906±0.017	0.614±0.014
0.424	0.563±0.021	0.556±0.020	0.670±0.015	0.442±0.013
0.474	0.421±0.016	0.437±0.016	0.532±0.011	0.343±0.012
0.523	0.342±0.014	0.325±0.015	0.411±0.012	0.239±0.009
0.574	0.244±0.010	0.246±0.011	0.304±0.009	0.188±0.007
0.624	0.192±0.010	0.196±0.010	0.250±0.009	0.143±0.007
0.674	0.155±0.008	0.161±0.009	0.198±0.008	0.126±0.007
0.724	0.115±0.007	0.136±0.008	0.164±0.007	0.108±0.007
0.774	0.085±0.006	0.106±0.010	0.137±0.007	0.075±0.005
0.825	0.061±0.005	0.091±0.010	0.112±0.008	0.069±0.007
0.873	0.053±0.006	0.076±0.010	0.100±0.009	0.054±0.008

Q^2 range covered by the two experiments: $\langle Q^2 \rangle$ = 2.5 GeV^2 for HERMES and $\langle Q^2 \rangle$ = 25 GeV^2 for EMC. The Q^2 range for the SLAC data is 1.8-8.5 GeV^2. Similar Q^2-dependent behaviour has been seen for hadrons in ref. [15]. In Figs. 7a and 7b the HERMES data have been evolved to the mean Q^2 of the EMC data using an NLO model for the evolution of the fragmentation functions [9]. The agreement between the evolved HERMES data and the EMC data is much improved, especially for π^0, demonstrating the need for QCD corrections. The comparison of multiplicities and fragmentation functions, and perhaps to a better extent the application to multiplicities of the model for the evolution of fragmentation functions, can be justified if isospin symmetry is assumed ($D_u^\pi = D_d^\pi$; where π represents the sum of positive and negative pions) and the strange quark contribution is neglected. In this case, the multiplicities are equivalent to the fragmentation functions. The effect of ignoring the strange quark can be inferred from a study in Ref. [26], where the effect of neglecting all sea quarks was estimated to be less than 10% (between 20% and 40%) for favoured (disfavoured) fragmentation functions. The dominance of u-quarks and the fact that the strange quark content is expected to be less than the light sea leads to the conclusion that the effect of the strange quarks should be well below 10%. On the other hand, the fact that the HERMES multiplicities are larger than the EMC fragmentation functions at low z, even after Q^2 corrections (see Fig. 7b) could indicate a failure of the above approximation, which is more likely at low z.

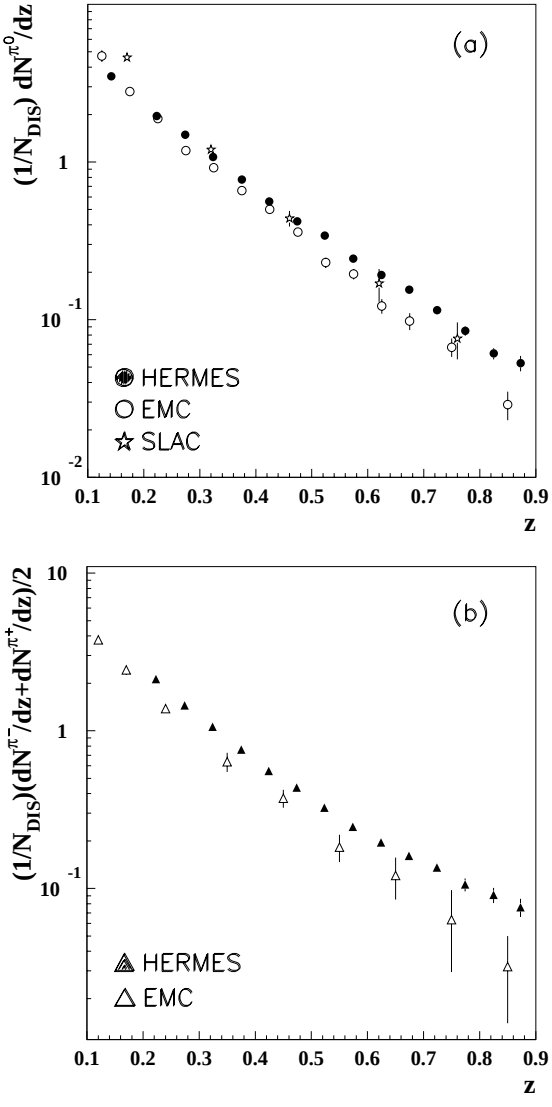

Fig. 6. a π^0 multiplicity from HERMES, EMC [18] and SLAC [19]. **b** Average charged pion multiplicity from HERMES compared to EMC fragmentation functions [20]. Only the statistical uncertainties are shown. The systematic uncertainties for neutral (charged) pions are 9% (7%) for HERMES, $\leq$ 15% for SLAC and $\leq$ 13% ($\leq$ 10%) for EMC

The charged pion multiplicities for HERMES are plotted in Fig. 8 as a function of x in four bins of z together with data on charged hadron multiplicities from EMC[3] [11]. All data have been evolved to Q^2= 2.5 GeV^2, the average Q^2 of HERMES, using the model described in the previous paragraph. The data are plotted at the measured x-value. The difference in the absolute value of the multiplicities is simply related to the fact that the HERMES data are for pions only while the EMC data are for hadrons. A significant x-dependence is seen, which gets stronger as z increases. The mean Q^2 per bin for HERMES varies only between 2.1 and 2.6 GeV^2. The observed

[3] The EMC pion data are not available in the required kinematic binning

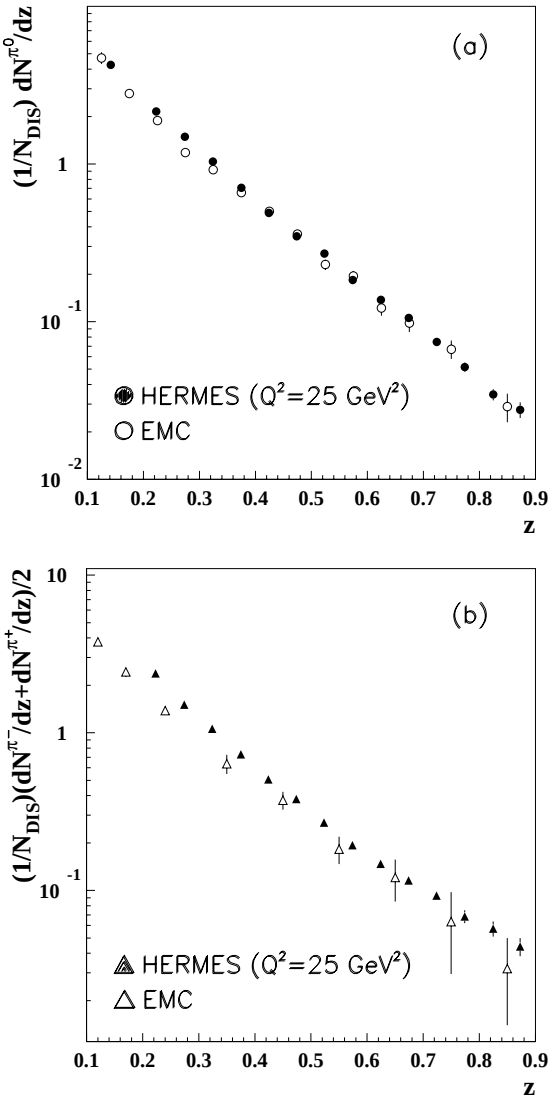

Fig. 7. Multiplicities for **a** neutral pions, and **b** the average of charged pions (note the EMC data for charged pions are for fragmentation functions). The HERMES results have been evolved to Q^2 =25 GeV^2 using a NLO QCD model [9]. Only statistical uncertainties are shown. The systematic uncertainties for neutral (charged) pions are 9% (7%) for HERMES and $\leq$ 13% ($\leq$ 10%) for EMC

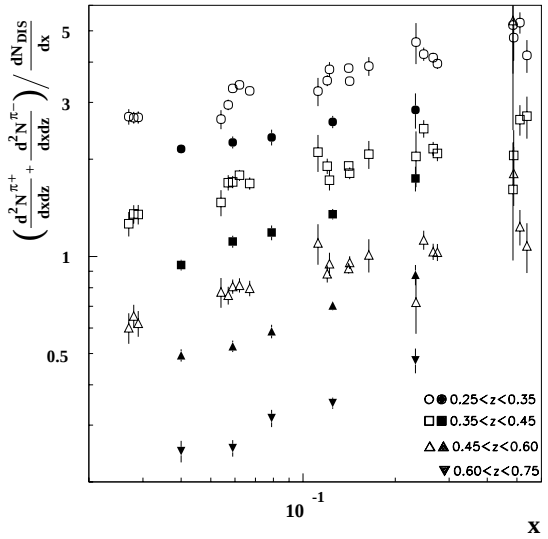

Fig. 8. Charged pion multiplicities $(\frac{d^2N^{\pi+}}{dx\,dz}+\frac{d^2N^{\pi-}}{dx\,dz})/\frac{dN_{DIS}}{dx}$ from HERMES (filled symbols) as a function of x in four different z-bins, compared to charged hadron multiplicities from EMC (open symbols). All data have been evolved to 2.5 GeV^2 and are plotted at the measured x-value

x-dependence is therefore not generated by the Q^2 correction. It is striking that the slopes in the data from both experiments are consistent even though they were measured at very different kinematics. E665 has also studied the x-dependence of hadron multiplicities [15]. While they conclude that there is no x-dependence for $x_F > 0.1$, these data are at lower x. In the (small) region of overlap with the HERMES data set, the E665 data do indeed show an x-dependence, although it is less pronounced.

The x-dependence is not expected to affect the Q^2 evolution of the data integrated over the measured x range. This is bourne out by the good agreement after NLO-QCD corrections of the two data sets for π^0 multiplicities in Fig. 7a. As stated earlier, the poorer agreement in Fig. 7b for charged pions could be due to the fact that multiplicities are compared to fragmentation functions in this case.

In order to better illustrate scaling violations in the fragmentation process, the Q^2-dependence of the data at fixed z was studied. For this analysis, only the data in the range $0.03 \leq x \leq 0.3$ were considered, to allow for a useful range of Q^2, which is quite limited by the HERMES acceptance for certain values of x. The total (neutral plus charged) pion multiplicity is plotted for 4 different z-bins in Fig. 9. The data show a clear Q^2-dependence, especially in the high z-bins. The variation of the data with Q^2 (i.e. the slope of the curves) is mostly in agreement with the Q^2-evolution predicted by the NLO QCD models [7–9]. It is worth mentioning that the above calculations are based on three analyses of fragmentation functions extracted from e^+e^- data taken at center of mass energies of 29 GeV [7] and of 29 and 91 GeV [8,9], i.e. at much higher energies than that of the data shown in Fig. 9. The sophistication of the parameterization increases for each successive version of the model, with the solid curve representing the most recent analysis. The absolute values of the present measurements are for the most part in reasonable agreement with the QCD predictions, considering that each theoretical calculation has an uncertainty of up to 15%, the systematic uncertainty on the data is 8.5%, and that data on multiplicities are compared to a parameterization of fragmentation functions.

4 Conclusion

Charged and neutral pion multiplicities in semi-inclusive deep-inelastic scattering at 27.5 GeV have been measured

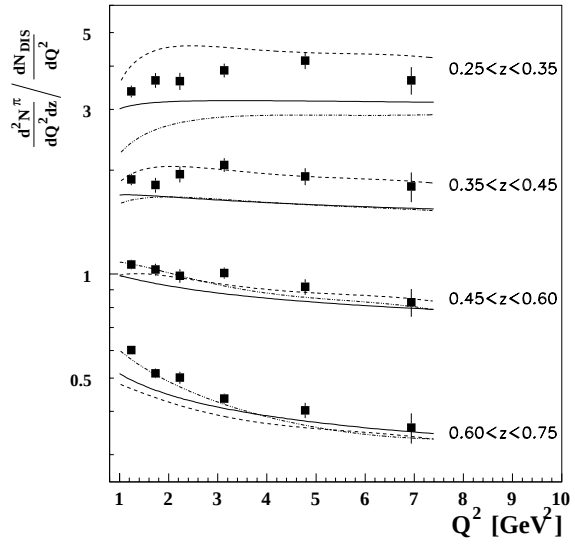

Fig. 9. Total (neutral plus charged) pion multiplicity $\frac{d^2N^\pi}{dQ^2\,dz} / \frac{dN_{DIS}}{dQ^2}$ as a function of Q^2 for various z-bins. The systematic uncertainty on the data is 8.5%. The three curves shown are NLO QCD calculations of fragmentation functions found in refs. [7] (dashed line), [8] (dotted line), and [9] (solid line)

by the HERMES collaboration. The multiplicities are consistent with isospin invariance below $z \sim 0.70$, and show that about 3/4 of the energy transferred in the scattering is carried by pions. These measurements provide data at lower Q^2 with improved statistical and systematic accuracies compared to earlier measurements. The agreement of the current results with previous data is improved, especially for π^0, when an NLO Q^2-evolution of the fragmentation process is taken into account. The Q^2-behaviour of the present data resembles that of the NLO QCD calculations. An observed x-dependence of the multiplicities is similar to previous results on hadron production from EMC when the data are evolved to the same Q^2.

Acknowledgements. We thank M. Greco, G. Kramer, and B. Pötter for useful discussions on fragmentation functions. We gratefully acknowledge the DESY management for its support and the staffs at DESY and the collaborating institutions for their significant effort. This work was supported by the Fund for Scientific Research-Flanders (FWO) of Belgium; the Natural Sciences and Engineering Research Council of Canada; the INTAS, HCM and TMR contributions from the European Community; the German Bundesministerium für Bildung, Wissenschaft, Forschung und Technologie (BMBF), the Deutscher Akademischer Austauschdienst (DAAD); the Italian Istituto Nazionale di Fisica Nucleare (INFN); Monbusho, JSPS, and Toray Science Foundation of Japan; the Dutch Stichting voor Fundamenteel Onderzoek der Materie (FOM); the UK Particle Physics and Astronomy Research Council; and the US Department of Energy and National Science Foundation.

References

1. J.F. Owens, Phys. Lett. **B76**, 85 (1978)
2. T. Uematsu, Phys. Lett. **B79**, 97 (1978)
3. R. Baier, K. Fey, Z. Phys. **C2**, 339 (1979)
4. N. Sakai, Phys. Lett. **B85**, 67 (1979)
5. P. Chiappetta et al., Nucl. Phys. **B412**, 3 (1994)
6. M. Greco, S. Rolli, A. Vicini, Z. Phys. **C65**, 277 (1995)
7. J. Binnewies, B.A. Kniehl, G.Kramer, Z. Phys. **C65**, 471 (1995)
8. J. Binnewies, B.A. Kniehl, G. Kramer, Phys. Rev. **D52**, 4947 (1995)
9. B. Kniehl, G. Kramer, B. Pötter, Nucl. Phys. **B582**, 514 (2000)
10. EMC Collaboration, J.J. Aubert et al., Phys. Lett. **B114**, 373 (1982)
11. EMC Collaboration, J. Ashman et al, Z. Phys. **C52**, 361 (1991)
12. P. Allen et al., Nucl. Phys. **B176**, 333 (1980)
13. ZEUS Collaboration, J. Breitweg et al., Eur. Phys. J. **C11**, 251 (1999)
14. H1 Collaboration, C. Adloff et al., Nucl. Phys. **B504**, 3 (1997)
15. E665 Collaboration, M.R. Adams et al., Z. Phys. **C76**, 441 (1997)
16. P. Allen et al., Nucl. Phys. **B214**, 369 (1983)
17. W. Wittek et al., Z. Phys. **C40**, 231 (1988)
18. EMC Collaboration, J.J. Aubert et al., Z. Phys. **C18**, 189 (1983)
19. T.P. McPharlin et al., Phys. Lett. **B90**, 479 (1980)
20. EMC Collaboration, M. Arneodo et al., Nucl. Phys. **B321**, 541 (1989)
21. EMC Collaboration, M. Arneodo et al., Z. Phys. **C31**, 1 (1986)
22. G. Drews et al., Phys. Rev. Lett. **41**, 1433 (1978)
23. P. Di Nezza, PhD thesis, Università di Perugia (1998); HERMES internal note 98-092. (www-hermes.desy.de/notes/pub/doc-public-index.html)
24. HERMES Collaboration, K. Ackerstaff et al., Nucl. Instr. and Meth. **A417**, 230 (1998)
25. F. Stock et al., Nucl. Instr. and Meth. **A343**, 334 (1994)
26. P. Geiger, PhD thesis, MPI Heidelberg (1998); HERMES internal note 98-005. (www-hermes.desy.de/notes/pub/doc-public-index.html)
27. H. Avakian et al., Nucl. Instr. and Meth. **A417**, 69 (1998)
28. G. Ingelman, A. Edin, J. Rathsman, Comp. Phys. Comm. **101**, 108 (1997)
29. T. Sjöstrand, Comp. Phys. Comm. **82**, 74 (1994)
30. GEANT Detector Description and Simulation Tool, CERN Program Library, Long Write-up W5014, 1994
31. H. Tallini, PhD thesis, University of Liverpool; HERMES internal note 98-024. (www-hermes.desy.de/notes/pub/doc-public-index.html)
32. I. Akushevich, N. Shumeiko, A. Soroko, Eur. Phys. J. **C10**, 681 (1999)
33. R.D. Field, R.P. Feynman, Phys. Rev. **D15**, 2590. (1977) The data used in the fit corresponding to the solid line in Fig. 5 are shown in Fig. 6 of this reference
34. L.L. Frankfurt, M.V. Polyakov, M. Strikman, M. Vanderhaeghen, Phys. Rev. Lett. **84**, 2589 (2000)
35. H. Avakian, Proceedings of the 8th International Workshop on Deep Inelastic Scattering and QCD (DIS 2000), Liverpool, England, Apr 25 - 30, 2000